Normal-Superfluid Interaction Dynamics in a Spinor Bose Gas

J. M. McGuirk,* D. M. Harber, H. J. Lewandowski,* and E. A. Cornell*

*JILA, National Institute of Standards and Technology and Department of Physics, University of Colorado,
Boulder, Colorado 80309-0440, USA*

Coherent behavior of spinor Bose-Einstein condensates is studied in the presence of a significant uncondensed (normal) component. Normal-superfluid exchange scattering leads to near-perfect local alignment between the spin fields of the two components. We observe that, through this spin locking, spin-domain formation in the condensate is vastly accelerated as the spin populations in the condensate are entrained by large-amplitude spin waves in the normal component.

A spinor Bose gas is a rich system for studying quantum coherence and the interaction dynamics of a superfluid with a normal component. The complex spin dynamics of such a system exhibits behavior that is not seen in either component individually. Mean-field effects, exchange scattering, and elastic collisions all may modify the local spin state of the components, while still preserving the ensemble-averaged spin. With these complicated interactions between the two components and within each component, it is often difficult to obtain readily interpretable results in the comingled normal-superfluid regime. An exception to this is the phenomenon of enhanced domain formation, in which the cooperative nature of normal-superfluid spin interaction is directly manifest. In this Letter, we describe the mechanism for enhanced domain formation and present data demonstrating the effect.

Interactions between condensates and normal components have been studied in great detail theoretically [1] and to a lesser extent experimentally [2]. An extra complication arises when the gas is comprised of multiple spin levels. Previous work with spinor condensates has primarily been concerned with the energetic and hydrodynamic properties of interpenetrating states with different longitudinal spin population, i.e., studies of spin-domain formation in mostly pure condensates [3–5]. There has been a small amount of work [6] devoted to studying properties of nearly pure spinor condensates involving their transverse spin, or internal coherence. In the fully nondegenerate limit, collective spin-wave behavior of a nondegenerate ensemble of ultracold atoms has been studied [7–9]. In this work, we study the regime in between nondegenerate spin waves and pure condensate spin-domain formation [10]. We present evidence of enhanced domain formation due to spin locking in a partially condensed system. Spin locking is the coherent spin dynamics which occur simultaneously and equivalently in both the normal component and the condensate. Exchange collisions act to constrain the spin of the condensate to that of the normal component, thus locally locking together the spins of the two components. The

result of this process is that spin domains can form in a condensate immersed in a normal gas up to 6 times faster than they do in a nearly pure condensate [11].

The spinor condensate used in this work consists of two sublevels within the ^{87}Rb ground state hyperfine manifold with identical magnetic moments, which form a pseudo-spin doublet that can be magnetically trapped [12]. We use the framework of the Bloch sphere to describe the spinor. Figure 1 indicates the coordinates used in this work.

At the low temperatures of this experiment, all interparticle interactions are of the spherically symmetric, s-wave type. These collisions lead to three primary effects.

(i) Momentum-changing elastic collisions: These may occur between two normal atoms, or between a normal and a condensate atom. Over relatively long time scales, these collisions enforce thermal equilibrium throughout the sample. They are not particularly relevant to the phenomena described in this paper, except in that they
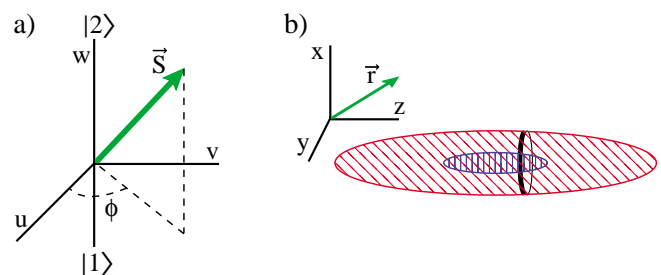

FIG. 1 (color online).   (a) Pseudospin coordinates, showing the vector $\vec{S}(\vec{r})$ and transverse phase angle ϕ. $\vec{S}(\vec{r}) = \pm \frac{1}{2}\hat{w}$ indicates that the spin population locally is in the pure $|2\rangle$ state and the $|1\rangle$ state, respectively, and ϕ is the phase of the internal coherence. (b) Real space coordinates. The actual aspect ratio of the normal cloud (angle hatch) and the embedded condensate cloud (vertical hatch) are a factor of 6 more elongated than shown in this figure. The high collision rate and rapid oscillation frequency in the radial $(x - y)$ directions ensure that the normal and condensate spins are uniform and aligned with each other within each circular cross section.

are necessary to generate the thermally equilibrated state that exists before the measurements begin.

(ii) Density-dependent mean-field potentials: The real parts of the forward and backward scattering amplitudes of the elastic collisions lead to a mean-field energy proportional to density. Because the scattering lengths a_{11} and a_{22} (where a_{ij} is the scattering length between spin states $|i\rangle$ and $|j\rangle$) differ by about 5%, the local density of atoms contributes to the energy splitting between the two spin projections. Therefore ϕ [13] is not uniform across the sample but depends on the local density [14].

(iii) Spin-rotation effect: When two colliding atoms are not perfectly spin aligned, there is a spin-rotation effect that arises from the coherent interference between a backscattered event and an unscattered event. As two atoms pass by each other, each atom's spin experiences a small rotation about the vector of their total spin. This effect occurs between two normal atoms, and between a normal and condensate atoms [10], but not between two condensate atoms, since condensate atoms are all in the same motional state. These collisions preserve total spin but can alter the spatial spin distribution.

The most readily accessible tool for studies of spinor gases, whether condensed or otherwise, is spin-domain formation. In a pure condensate, for instance, the interaction energies of the two states are slightly different, and therefore it is energetically favorable in trap for the condensate to form spin domains (if the intraspecies scattering lengths are not significantly greater than the interspecies scattering length) [14]. This behavior was shown to be the case for ^{87}Rb [5]. In a pure condensate, the driving mechanism for the spin transport comes from the spatial inhomogeneity of the relative mean-field shift of the two spin states. This produces a spatial gradient in the phase, ϕ. In a condensate, which is a single wave function, a gradient in the relative phase of the spin states means perforce there is a relative velocity between the two states, given by $u(z) = (\hbar/m)\nabla\phi(z)$ [15]. However, as described below, this mechanism of spin transport is relatively unimportant in condensates when a significant normal component is present.

The spin dynamics of condensates with large normal components are instead dominated by spin waves in the normal component. Condensates themselves do not support spin waves due to the absence of the spin-rotation effect described above, but spin locking to the spin wave in the normal component vastly accelerates domain formation by using exchange scattering as a mechanism for spin transport. This process is illustrated in Fig. 2. With all the spins in the ensemble initially rotated uniformly into the u-v plane, ϕ begins to evolve nonuniformly because of the spatial inhomogeneity in the potential, leading to a spatial phase gradient, which in turn produces spin waves in the normal component [8,9]. Spin waves occur as a number of spin rotating collisions between normal-component atoms with slightly different spins (due to the inhomogeneity of the potential) produce a macroscopic spin current, which drives spatiotemporal spin oscillations. For the large density inhomogeneities typical in this work, spin waves are strongly driven outside of the linear regime, leading to oscillation frequencies dependent on the driving amplitude [16]. During the progression of the spin wave, the condensate and normal components undergo exchange scattering that locally equilibrates their spins, thereby entraining the condensate spin dynamics in the normal-component spin wave. The highly overdriven spin wave causes rotation of the normal-component spin vectors (and thus the condensate also) out of the u-v plane on an even faster time scale than spin waves above T_c.

The experiment uses ^{87}Rb atoms in a hybrid Ioffe-Pritchard magnetic trap ({7, 230, 230} Hz frequencies) that are cooled to degeneracy by radiofrequency evaporation [17]. The final temperature is adjusted to values ranging from above T_c to $T/T_c < 0.3$ [18]. The condensate number was kept constant at $\sim 6.5 \times 10^4$, a relatively small number chosen to limit dipolar relaxation in $|2\rangle$. Each experimental cycle begins with an ensemble in $|1\rangle$, $S(\vec{r}) = -\frac{1}{2}\hat{w}$. A $\pi/2$ pulse then rotates all spin vectors to lie entirely in the transverse u-v plane, creating an equal coherent superposition of $|1\rangle$ and $|2\rangle$ [19]. The spinor system is allowed to evolve, and the resulting spatial spin distribution is probed. The longitudinal spin component $S_w(\vec{r})$ is measured by independently imaging the $|1\rangle$ and $|2\rangle$ states of the superposition. ϕ is measured by applying a second $\pi/2$ pulse to create Ramsey fringes [9].
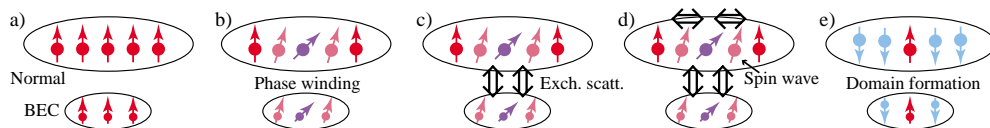

FIG. 2 (color online). Schematic explanation of how normal-superfluid spin locking leads to rapid domain formation. The normal and condensate components are spatially offset for clarity. (a) Immediately after a $\pi/2$ pulse, the spin is aligned all along the sample in both components. (b) Mean field effects within each component, and between the components, cause density-dependent evolution of ϕ. Although the density is much higher in the condensate, (c) exchange scattering keeps the spins of both components locked at each location along the axis. (d) Axial gradients in ϕ launch large-amplitude spin waves through the normal component. Exchange collisions continue to ensure that the condensate and normal component spin fields are locally aligned so that (e) spin domains form rapidly and simultaneously in both components.
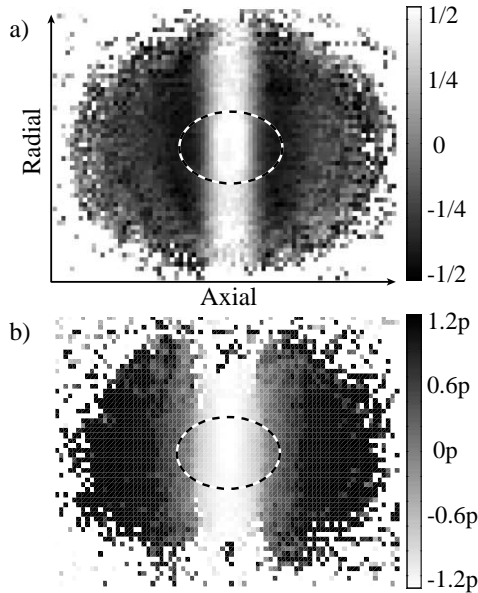
FIG. 3. (a) Longitudinal spin profile at $T/T_c = 0.8$ after a 50 ms evolution time: $S_w(\vec{r}) = \frac{1}{2}[N_2(\vec{r}) - N_1(\vec{r})]/[N_2(\vec{r}) + N_1(\vec{r})]$, calculated from the measured $|1\rangle$ and $|2\rangle$ state populations. White and black shading represent $S_w(\vec{r}) \approx \pm\frac{1}{2}$, respectively (atoms predominantly in $|2\rangle$ and $|1\rangle$, respectively). The white areas near the edges of each image are a mask for areas where there is not enough signal to determine accurately $S_w(\vec{r})$. (b) Corresponding spin profile showing the transverse phase angle ϕ, obtained from Fourier transforms of Ramsey fringes at each two-dimensional spatial bin. The dotted lines show the Thomas-Fermi radius of the condensate. The spins of the condensate and normal component are well aligned as seen by the radial homogeneity; there is no signature of the condensate in the spin profile, despite the tendency for $\dot{\phi}$ to be different between condensate and normal component due to differences in mean-field effects.

The imaging is accomplished after expansion by destructive absorptive imaging. Figure 3 shows two-dimensional spin reconstructions for a partially condensed ensemble. Because the condensate component is significantly more compact than the normal component, it is possible to distinguish the two components by their location in the radial direction. One can thus separately observe the spin dynamics in the condensate and in the normal gas.

The intercomponent dynamics are elucidated in Fig. 4. Figure 4(a) shows domain formation in a mostly pure condensate ($T/T_c = 0.3$). The $|2\rangle$ state forms a domain in the center of the trap, and the $|1\rangle$ state moves to the outside, as described above. The time scale for this motion is ~280 ms for a condensate with number density $\sim10^{14}$ cm^{-3}. The other end of the temperature range is shown in Fig. 4(c), where spin waves in a cloud just above degeneracy ($T/T_c = 1.1$) are depicted. The maximum spin rotation out of the u-v plane, equivalently the peak of spin-domain formation, occurs at ~120 ms.

The spin dynamics for a partially condensed system are strikingly different. An ensemble at $T/T_c = 0.8$ is shown in Fig. 4(b). The condensate inhabits the center third of each image, and the normal component is spread throughout the entire image. The first point to note is the uniformity of the images in the radial direction, which shows spin locking, i.e., $S_w(\vec{r})$ is only a function of the axial position z. Second, in the presence of the extra driving potential caused by the condensate, the normal-component spin wave has a frequency approximately twice as high as the less strongly driven nondegenerate case. The last important feature of this data is that spin domains form in the condensate at the same time as the spin wave rotates the normal-fluid spin out of the u-v plane. Domain formation occurs almost 6 times faster when driven by condensate-normal component exchange scattering than without the normal-component present.

At still later times, as the normal component decoheres, spin-wave phenomena become less pronounced, and the normal component relaxes to a homogeneous spin distribution. Empirically, the $|2\rangle$ state decays and leaves the trap at a rate comparable to normal-cloud decoherence, complicating the observation of steady-state behavior.
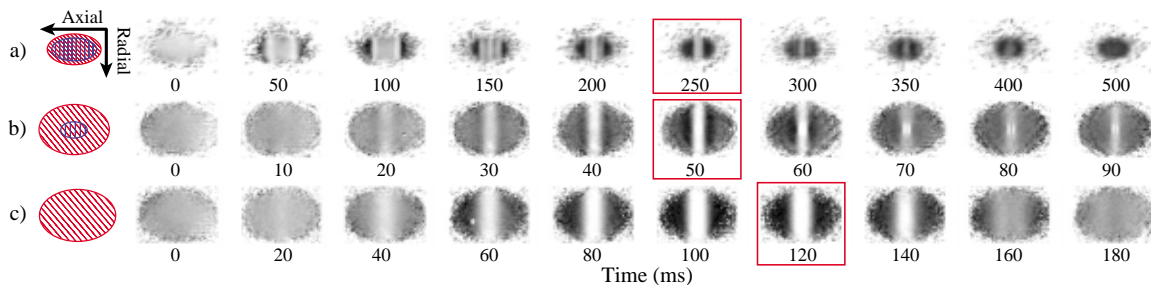
FIG. 4 (color online). Temporal evolution of $S_w(\vec{r})$ for $T/T_c = $ (a) 0.3, (b) 0.8, and (c) 1.1. The shading scale for each image is identical to Fig. 3(a). The first image of each row shows the fitted size of the condensate (vertical hatch) and the normal component (angle hatch). In (b), the condensate occupies the center third of each image, while it dominates the image in (a) and is not present in (c). The time scale to reach the maximum spin domain formation (boxed images) is highly accelerated when there is a significant normal component present as in (b) and is even faster than in (c) due to the extra energy inhomogeneity from the mean field shift of the condensate. Images are 120 μm across in (a) and 300 μm in (b) and (c).

The formation of spin domains in pure condensates, driven by gradients in mean-field potentials, is an effect that was observed six years ago [4,5], and this basic effect is seen again in Fig. 4(a). It is tempting to think of the rapid condensate spin-domain formation seen in Fig. 4(b) as simply an accelerated version of the same physical process. For instance, the thermal cloud might be contributing to the axial gradient of the mean-field potential, such that $\phi(z)$ in the condensate develops a large gradient more quickly, with a corresponding larger relative superfluid velocity between the two spin projections. We have ruled out this explanation through a quantitative study of the evolution of $\phi(z)$ in the condensate. The observed $\partial\phi/\partial z$ gives the rate of *potential-driven* relative flow of the two spin projections, while the divergence of this flow, $\partial^2\phi/\partial z^2$, would be proportional to the rate at which the local value of S_w evolves towards a pure $|1\rangle$ or $|2\rangle$ projection. Indeed, this analysis can account within a factor of 1.5 for the rate of spin-domain formation in the case of the near-pure condensate shown in Fig. 4(a). However, the potential-driven superfluid flow measured within the condensate for the conditions corresponding to the mixed-case example of Fig. 4(b) are too small by a factor of 40 to account for the observed spin-domain formation rate $\dot{S}_w$. Obviously then, the spin dynamics of the condensate, which cannot support its own spin wave, arises predominantly from interactions with the normal-cloud spin wave.

In conclusion, we have studied normal-superfluid spinor interactions in a regime in which the (normally highly complex) effects admit a simple interpretation. To complement the dynamics presented here, a study of the causes and effects of spin decoherence in a partially condensed system will be the topic of a future publication.

---

*Quantum Physics Division, National Institute of Standards and Technology.

[1] See, for instance, M. Guilleumas and L. P. Pitaevskii, Phys. Rev. A **61**, 013602 (2000); U. Al Khawaja and H T. C. Stoof, Phys. Rev. A **62**, 053602 (2000); M. J. Davis, S. A. Morgan, and K. Burnett, Phys. Rev. A **66**, 053618 (2002); J. E. Williams, T. Nikuni, and C. W. Clark, Phys. Rev. Lett. **88**, 230405 (2002); K. Goral, M. Gajda, and K. Rzazewski, Phys. Rev. A **66**, 051602 (2002); B. Jackson and E. Zaremba, Phys. Rev. Lett. **88**, 180402 (2002).

[2] D. S. Jin *et al.*, Phys. Rev. Lett. **78**, 764 (1997); D. M. Stamper-Kurn *et al.*, Phys. Rev. Lett. **81**, 500 (1998); I. Bloch, T. W. Hänsch, and T. Esslinger, Nature (London) **403**, 166 (2000); O. M. Maragò, G. Hechenblaikner, E. Hodby, and C. J. Foot, Phys. Rev. Lett. **86**, 3938 (2001); S. Dettmer *et al.*, Phys. Rev. Lett. **87**, 160406 (2001).

[3] T. L. Ho, Phys. Rev. Lett. **81**, 742 (1998).

[4] J. Stenger *et al.*, Nature (London) **396**, 345 (1998).

[5] D. S. Hall *et al.*, Phys. Rev. Lett. **81**, 1539 (1998).

[6] M. R. Matthews *et al.*, Phys. Rev. Lett. **83**, 3358 (1998).

[7] A. Leggett and M. Rice, Phys. Rev. Lett. **20**, 586 (1968); E. P. Bashkin, JETP Lett. **33**, 8 (1981); C. Lhuillier and F. Laloë, J. Phys. (Paris) **43**, 197 (1982); **43**, 225 (1982); K. Miyake, W. Mullin, and P. C E. Stamp, J. Phys. (Paris) **46**, 663 (1985); L. P. Lévy and A. E. Ruckenstein, Phys. Rev. Lett. **52**, 1512 (1984); N. P. Bigelow, J. H. Freed, and D. M. Lee, Phys. Rev. Lett. **63**, 1609 (1989).

[8] M. Ö. Oktel and L S. Levitov, Phys. Rev. Lett. **88**, 230403 (2002); J. N. Fuchs, D. M. Gangardt, and F. Laloë, Phys. Rev. Lett. **88**, 230404 (2002); J. E. Williams, T. Nikuni, and C. W. Clark, Phys. Rev. Lett. **88**, 230405 (2002); A. S. Bradley and C. W. Gardiner, J. Phys. B **20**, 4299 (2002).

[9] J. M. McGuirk *et al.*, Phys. Rev. Lett. **89**, 090402 (2002).

[10] T. Nikuni and J. E. Williams, cond-mat/0304095.

[11] The effects discussed in this paper also may be relevant to the interpretation of the ultraviolet spectrum of degenerate atomic hydrogen (see D. G. Fried *et al.*, Phys. Rev. Lett. **81**, 3811 (1998); M. Ö. Oktel and L. S. Levitov, Phys. Rev. Lett. **83**, 6 (1999)].

[12] The two spin states in question are the hyperfine states $|1\rangle \equiv |F = 1, m_F = -1\rangle$ and $|2\rangle \equiv |F = 2, m_F = 1\rangle$ of the $5S_{1/2}$ manifold. This pseudospin doublet can be thought of as a spin-$\frac{1}{2}$ system.

[13] The mean field-driven phase evolution of the system is determined from the local density n of the components as follows:

$$\dot{\phi}_{\text{norm}} = \frac{4\pi\hbar(a_{11} - a_{22})}{m}(2n_{\text{norm}} + 2n_{\text{cond}}),$$

$$\dot{\phi}_{\text{cond}} = \frac{4\pi\hbar(a_{11} - a_{22})}{m}(2n_{\text{norm}} + n_{\text{cond}}).$$

[14] The interspecies scattering length a_{12} for the two spins is nearly exactly the geometric mean of the two intraspecies scattering lengths, a_{11} and a_{22}. This equality means that density-dependent effects on $\dot{\phi}$ are independent of the spin tipping angle. It also means that the tendency of a $T = 0$ spinor condensate to form spin domains spontaneously is driven not by the inherent immiscibility of the spins, but by the energy minimization associated with moving one spin species to regions of the cloud with high density and the other to regions of low density [see E. A. Cornell *et al.* J. Low Temp. Phys. **113**, 151 (1998)].

[15] F. Dalfovo, S. Giorgini, L. P. Pitaevskii, and S. Stringari, Rev. Mod. Phys. **71**, 463 (1999).

[16] J. N. Fuchs, D. M. Gangardt, and F. Laloë, Eur. Phys. J. D **25**, 57 (2003).

[17] H. J. Lewandowski, D. M. Harber, D. L. Whitaker, and E. A. Cornell, J. Low Temp. Phys. **132**, 309 (2003).

[18] All values of T/T_c have been adjusted for interaction and finite-number effects (see [15]), but for $T/T_c \lesssim 0.35$ it is difficult to determine temperature accurately.

[19] The spin of the system is manipulated using a two-photon coupling pulse [9], with ~3 kHz effective Rabi frequency.